



## Thermal escape of carbon from the early Martian atmosphere

Feng Tian,<sup>1</sup> James F. Kasting,<sup>2</sup> and Stanley C. Solomon<sup>3</sup>

Received 29 October 2008; revised 10 December 2008; accepted 31 December 2008; published 31 January 2009.

[1] Observations suggest that Mars was wet and warm during the late Noachian, which probably requires a dense CO<sub>2</sub> atmosphere. But would a dense CO<sub>2</sub> early Martian atmosphere have been stable under the strong EUV flux from the young Sun? Here we show that thermal escape of carbon was so efficient during the early Noachian, 4.1 billion years ago (Ga), that a CO<sub>2</sub>-dominated Martian atmosphere could not have been maintained, and Mars should have begun its life cold. By the mid to late Noachian, however, the solar EUV flux would have become weak enough to allow a dense CO<sub>2</sub> atmosphere to accumulate. Hence, a sustainable warm and wet period only appeared several hundred million years (Myrs) after Mars formed. **Citation:** Tian, F., J. F. Kasting, and S. C. Solomon (2009), Thermal escape of carbon from the early Martian atmosphere, *Geophys. Res. Lett.*, 36, L02205, doi:10.1029/2008GL036513.

[2] Geomorphological and geochemical features suggest that Mars was wet and relatively warm during the latter part of the Noachian period, which ended ~3.7 Ga [Baker, 2001; Jakosky and Phillips, 2001; Solomon et al., 2005]. The early Noachian has less evidence for fluvial modification—a change that could be caused either by a colder climate or simply by lack of preservation [Phillips et al., 2001]. To keep the global mean surface temperature of early Mars above the freezing point of water requires 1–5 bars of CO<sub>2</sub> [Kasting, 1991; Forget and Pierrehumbert, 1997], although it has yet to be demonstrated that this mechanism actually works for plausible assumptions about CO<sub>2</sub> cloud cover [Mischna et al., 2000]. One view of the early Martian climate is that the surface conditions were warm enough during the Noachian for the existence of stable liquid water and became colder in the following epochs as a consequence of massive loss of its atmosphere. Alternatively, the warm periods could have been short and were the results of large impacts [Segura et al., 2002].

[3] In this work we use a newly developed 1-D, multi-component, hydrodynamic, planetary thermosphere-ionosphere model [Tian et al., 2008a, 2008b], in which an electron transport-energy deposition model (GLOW) is coupled to the thermosphere-ionosphere model. This approach allowed us to self-consistently calculate ionization and excitation rates of thermospheric constituents, along with the associated ambient electron heating rates, therefore avoid making arbitrary assumptions about EUV heating

efficiencies. In order to apply the model to a CO<sub>2</sub>-dominated upper atmosphere, electron impact cross sections [Sawada et al., 1972] for both CO<sub>2</sub> and CO were added to the GLOW model, and atomic carbon chemistry reactions from Fox and Sung [2001] were included. The model includes radiative cooling from the CO<sub>2</sub> 15- $\mu$ m band [Gordiets et al., 1982], the NO 5.7- $\mu$ m band [Kockarts, 1980], and the atomic oxygen fine structure 63- $\mu$ m band [Glenar et al., 1978]. In addition, we include CO 4.7- $\mu$ m band cooling by employing the Einstein A-coefficient expressions in Chin and Weaver [Chin and Weaver, 1984], using an average value of 16.3 s<sup>-1</sup> for all rovibrational transitions between  $v = 1$  and  $v = 0$  states. The model evaluates the altitude of the exobase level and adjusts the upper boundary accordingly. At the upper boundary the model uses the Jeans escape formula, including the contribution of the bulk motion velocity, to calculate the effusion velocities of the various species and then weighs them by their respective mass mixing ratios to determine the bulk motion velocity at the top of the model atmosphere.

[4] The model was first applied to the thermospheres of both present Mars and present Venus under solar mean conditions. Figure 1 shows that the model-calculated neutral temperature and mass density profiles are similar to the Martian upper atmospheric structure at midlatitudes under both summer solstice (Ls = 90) and winter solstice (Ls = 270) conditions [Stewart, 1987]. Figure 2 shows that the model-calculated neutral temperature and mass density profiles agree with the upper atmospheric structure in a global empirical model of present Venus [Hedin et al., 1983].

[5] When extrapolating the model to early Mars, the solar EUV energy fluxes are assumed to follow the expression by Ribas et al. [2005]:  $F = 29.7 \cdot t^{-1.23}$  ergs cm<sup>-2</sup> s<sup>-1</sup>, where  $t$  is the stellar age in billions of years. Solar EUV fluxes are 10 $\times$  and 20 $\times$  the present level at 3.8 and 4.1 Ga, respectively, and the fluxes were corrected for Mars' orbital distance.

[6] Figure 3 shows the temperature and density profiles of calculated early Martian upper atmospheres. The colors of the curves represent different solar EUV energy fluxes (blue: 3 $\times$  present EUV, green: 10 $\times$ , red: 20 $\times$ ). The solid curves assume the same lower atmosphere as that of present Mars (surface pressure  $p_s = 6$  mbar). The dashed and dot-dashed curves assume 1-bar and 3-bar CO<sub>2</sub>-dominated atmospheres, respectively. The lower boundary altitudes in the dense atmosphere cases are adjusted so that the densities are comparable to those in the 6-mbar atmosphere cases. Despite the differences in the lower thermospheres (<300 km), the behavior of the upper thermospheres is similar in all three different surface pressure cases. In the following, we only distinguish the calculations by the solar EUV energy flux (Case 1 = 3 $\times$ , Case 2 = 10 $\times$ , Case 3 = 20 $\times$ ) and we only discuss the 3-bar atmosphere calculations. The

<sup>1</sup>Department of Earth, Atmospheric, and Planetary Sciences, MIT, Cambridge, Massachusetts, USA.

<sup>2</sup>Department of Geosciences, Pennsylvania State University, University Park, Pennsylvania, USA.

<sup>3</sup>High Altitude Observatory, National Center for Atmospheric Research, Boulder, Colorado, USA.

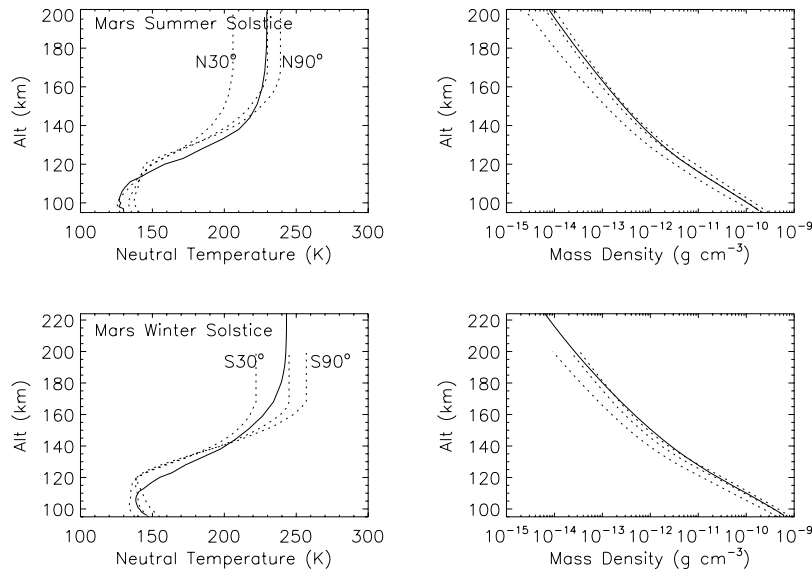


**Figure 1.** Validation of the model in the present Martian atmosphere. The dotted curves are the empirical temperature and mass density profiles ((top) summer solstice and (bottom) winter solstice) at latitude 90, 60, and 30 degrees, respectively [Stewart, 1987]. The solid curves are the model-calculated temperature/mass density profiles.

dotted curves in the right panel are the density profiles of CO<sub>2</sub> and atomic carbon in case 3.

[7] The calculated exobase temperature and altitude in Case 1 were approximately 400 K and 400 km. The ability of a gas to escape thermally from early Mars can be measured by the Jeans escape parameter:  $\lambda = \frac{GMm}{kTr}$ , where  $G$  is the gravitational constant,  $M$  is the mass of the planet,  $m$  is the mass of escaping particle,  $k$  is the Boltzmann constant, and  $T$  and  $r$  are the temperature and radial distance at the exobase. The Jeans escape parameter for atomic oxygen was 54 in case 1, implying that it would not have escaped thermally. In Case 2, the exobase expanded to approximately 900 km altitude and the exobase temperature rose to 800 K. Consequently,  $\lambda_o$  dropped to 23, still too large to permit efficient thermal escape. The Martian upper atmosphere was significantly warmer and more expanded in Case 3. The exobase altitude reached  $\sim 10,000$  km with temperature  $>2500$  K - a nonlinear increase of the exobase temperature with increasing solar EUV flux similar to that found in earlier studies [Smithro and Sojka, 2005; Tian et al., 2008a, 2008b] - and both atomic oxygen and carbon were abundant at this height. One reason for the nonlinear response is that the main IR cooling agents, such as CO<sub>2</sub>, are destroyed by the high EUV flux, so that cooling

decreases as EUV level increases [Smithro and Sojka, 2005]. The escape parameters for C and O were  $\lambda_c = 1.8$  and  $\lambda_o = 2.4$ , low enough to allow these species to readily escape. The weak gravity field of Mars was thus no match for the extreme solar EUV energy input from the early young Sun. In contrast, Earth and Venus, with their stronger gravity, remained well protected when exposed to  $<40\times$  present Earth EUV levels (F. Tian and S. Seager, On the stability of super Earth atmospheres, submitted to *Astrophysical Journal Letters*, 2008). Energy analysis shows that the cooling caused by adiabatic expansion dominates the energy budget in Case 3, indicating that the Martian thermosphere was well within the hydrodynamic regime [Tian et al., 2008a, 2008b].

[8] In principle, when solar EUV heating is strong and temperatures are high, CO<sub>2</sub> could efficiently cool the thermosphere through its 4.3- $\mu\text{m}$  emission. However, the region ( $<200$  km altitude) where the CO<sub>2</sub> density is high remains cold (Figure 3), which should make the CO<sub>2</sub> 4.3- $\mu\text{m}$  IR cooling relatively unimportant.

[9] We next applied our model to different times in Mars' history, using the estimated EUV enhancements by Ribas et al. [2005]. The calculated thermal escape flux of carbon atoms from the Martian atmosphere was  $\sim 10^{11}$  cm<sup>-2</sup> s<sup>-1</sup> at

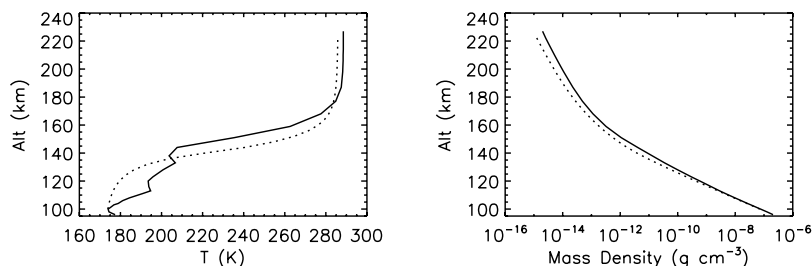


**Figure 2.** Validation of the model in the present Venusian atmosphere. Dotted curves are the model-calculated temperature/mass density profiles. Solid curves are those in a global empirical model of Venus [Hedin et al., 1983].

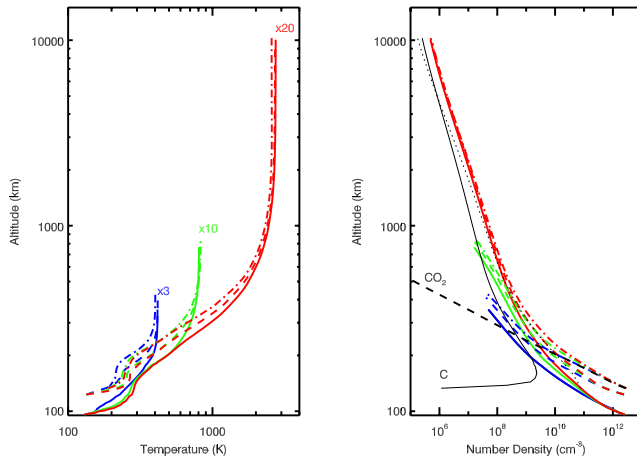


**Figure 3.** The calculated upper atmospheric structure of early Mars: (left) neutral temperature profiles and (right) number density profiles. Blue, green, and red colors represent different solar EUV energy flux levels. Curve styles represent different atmospheric pressures. The black curves in Figure 3 (right) are the number density profile of CO<sub>2</sub> (dashed), atomic carbon (solid), and atomic oxygen (dotted) in Case 3.

4.1 Ga (dashed curve in Figure 4) and could have reached  $10^{12} \text{ cm}^{-2} \text{ s}^{-1}$  at 4.5 Ga. The corresponding timescales required to lose 1 bar of CO<sub>2</sub> from Mars ( $3.7 \times 10^{43}$  carbon atoms) are 10 and 1 Myrs respectively. Hence, these dense atmospheres could not have been maintained during the early Noachian unless the loss of CO<sub>2</sub> was balanced by rapid rates of volcanic outgassing.

[10] We estimate CO<sub>2</sub> outgassing rates on Mars during the early Noachian in the following manner: At present, both Earth and Venus have about 100 bar of CO<sub>2</sub> at their surfaces. On Venus, it is in the atmosphere; on Earth, it is mostly in carbonate rocks. 100 bar of CO<sub>2</sub> on the Earth is  $\sim 7 \times 10^{45}$  molecules. Mars has about 1/10th of Earth's mass, 1/5th of Earth's surface area, and 40% of Earth's gravity. Hence, if Mars was formed from the same material as Earth, its total CO<sub>2</sub> reservoir could have been as much as  $7.5 \times 10^{44}$  molecules, or 20 bars. This is consistent with the estimate based on geomorphology [Carr, 1986]. Considering that Mars formed farther from the Sun than the Earth and thus could contain materials with volatile content  $2 \times$  richer than Earth, a maximum 40-bar ( $1.5 \times 10^{45}$  molecules) total CO<sub>2</sub> inventory is possible. If most of Mars' CO<sub>2</sub> were emplaced in its atmosphere at 4.5 Ga, immediately following the planet's formation, the entire inventory could have been lost within 40 Myrs.

[11] Alternatively, Mars could have released CO<sub>2</sub> gradually and thus avoided the initial fast volatile loss episode. It is estimated that  $\sim 1.5$  bar of CO<sub>2</sub> was released volcanically through the formation of the Tharsis bulge during the late Noachian [Phillips et al., 2001]. This estimate is based on the assumption that the CO<sub>2</sub> content in the Tharsis magmas is the same as that of Hawaiian basalts. If Martian magma contains more volatiles, 3 bar of CO<sub>2</sub> could have been released by the Tharsis system. If we assume that the outgassing rate decayed exponentially from 4.56 billion years ago and use 40 bars as the total CO<sub>2</sub> inventory and

3 bars as the Tharsis CO<sub>2</sub> inventory, the upper solid line in Figure 4 is obtained. The lower solid line in Figure 4 is for 20 bars as the total CO<sub>2</sub> inventory and 1.5 bars as the Tharsis CO<sub>2</sub> inventory. For purposes of comparison, the dot-dashed line marks the CO<sub>2</sub> outgassing rate for present Earth [Sleep and Zahnle, 2001]. By these estimates, this is roughly equal to the Martian outgassing rate at  $\sim 4$  Ga. Using these assumptions of the outgassing history, carbon loss rate from Mars was greater than the CO<sub>2</sub> outgassing rate throughout the early Noachian - a dense early Noachian Martian atmosphere could not have been formed. Outgassing of CO<sub>2</sub> might have been episodic instead of continuous. Nevertheless, considering the short time scale (1–10 Myrs for 1 bar CO<sub>2</sub>) for carbon to escape from early Mars, the total time during which a dense CO<sub>2</sub> atmosphere could have been maintained prior to 4.1 Ga should have been brief.

[12] Because of Mars' weak gravity, the planet could also have lost significant atmosphere through impact erosion [Melosh and Vickery, 1989], which could have further reduced the total CO<sub>2</sub> inventory. This only strengthens our conclusion that Mars could not have sustained a dense CO<sub>2</sub> atmosphere for time scale of  $\sim 10$  Myrs, and thus was initially cold. (With few greenhouse gases present, the

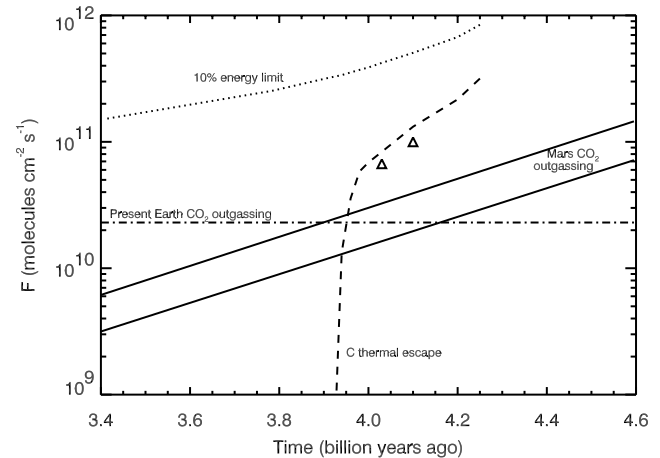


**Figure 4.** Comparison between atmospheric escape and outgassing on early Mars. The dashed curve represents the thermal escape flux of atomic carbon from a CO<sub>2</sub>-dominated atmosphere. The triangles represent the thermal escape fluxes of carbon from an atmosphere with an H<sub>2</sub> mixing ratio of  $(3-5) \times 10^{-4}$  and with associated H escape fluxes of the order of  $10^{10} \text{ cm}^{-2} \text{ s}^{-1}$ . The two solid lines represent possible CO<sub>2</sub> volcanic outgassing fluxes on early Mars. The dash-dotted horizontal line marks CO<sub>2</sub> outgassing flux ( $6 \times 10^{12}$  moles per year, or  $2.3 \times 10^{10} \text{ cm}^{-2} \text{ s}^{-1}$ ) on the present Earth. The dotted curve represents 10% of the energy-limited escape flux of carbon,  $F_{\text{lim}} = \frac{\varepsilon F_{\text{EUV}}}{4E_{\text{grav}}}$ , where  $F_{\text{EUV}}$  is 11.04 the solar EUV energy flux ( $\text{ergs cm}^{-2} \text{ s}^{-1}$ ),  $E_{\text{grav}} = GMm/r$  ( $\text{ergs}$ ) is the potential energy of one single escaping particle,  $\varepsilon$  includes both the heating efficiency (the conversion factor between the absorbed solar EUV energy and the thermal energy,  $<1$ ) and the altitude variation of energy absorption ( $>1$ ). Here,  $\varepsilon$  is set to be unity. The factor of 4 accounts for the difference between the solar energy absorption area and the surface area of the planet.

effective surface temperature would have been  $\sim 195$  K for a solar constant of 0.7 times present and a surface albedo of 0.2.) The calculations presented so far neglect nonthermal escape processes, as the velocities of multiple gases are specified at the exobase according to the Jeans escape formula.

[13]  $\text{H}_2$  should also have been released into the atmosphere by early Martian volcanoes, and so we must ask whether this would affect our calculations. On the modern Earth, the ratio of  $\text{H}_2/\text{CO}_2$  in volcanic gases is  $\sim 0.1$  to 1 [Holland, 2002; Canfield *et al.*, 2006]. In a reducing or neutral atmosphere,  $\text{H}_2$  released from volcanoes should be largely balanced by its loss to space [Kasting, 1993; Tian *et al.*, 2005]. Simulations with  $\text{H}_2$  mixing ratios of  $(3-5) \times 10^{-4}$ , similar to those expected on early Earth [Kasting, 1993], produced hydrogen escape fluxes of  $(1-2) \times 10^{10} \text{ cm}^{-2} \text{ s}^{-1}$  and slightly reduced the carbon escape fluxes (marked as triangles in Figure 4).

[14] The calculated thermal escape rate of atomic carbon from early Noachian Mars is faster than that of atomic oxygen because C is lighter and its abundance near the exobase is comparable to that of O. Thus, Mars should have gained  $\text{O}_2$  in its atmosphere over time at a rate proportional to the excess of C escape over that of O. Simply balancing the rate of C escape with half that of O (so that  $\text{CO}_2$  effectively escapes) in the  $20\times$  present EUV case yields an  $\text{O}_2$  mixing ratio of  $\sim 2\%$ . Whether any net  $\text{O}_2$  would have accumulated depends on the relative rate of  $\text{H}_2$  outgassing compared to net loss of C over O, which requires future study. A further complication is the uncertain abundance of CO in the lower atmosphere. A recent photochemical model for Mars early atmosphere [Zahnle *et al.*, 2008] showed that a 1-bar  $\text{CO}_2$  atmosphere could be photochemically converted into CO over the timescale of 0.1 to 1 Gyrs—a phenomenon that has been recognized for over 30 years [McElroy, 1972]. We note that this timescale is much shorter than the carbon loss timescale during the early Noachian, which suggests that a  $\text{CO}_2$  atmosphere could be more unstable than that considered by Zahnle *et al.* [2008]. On the other hand, this “CO runaway” could be prevented either by buildup of  $\text{O}_2$ , as just mentioned, or by catalytic recombination of CO with oxidants on the Martian surface.

[15] Although we have not calculated this explicitly, the thermal escape of C and O should have fractionated their isotopes so that heavier isotopes were preferentially retained. Indeed, modest enrichments of the heavier isotopes of C and O are observed in the present Martian atmosphere [Jakosky and Phillips, 2001; Krasnopolsky *et al.*, 2007]. Because atmosphere diffusive separation, escape, and the exchange of atmospheric gases with the regolith, crust, and polar caps all contribute to the isotopic fractionation history [Jakosky and Phillips, 2001], the connection between the isotopic pattern observed in present Mars atmosphere and the planet’s atmosphere loss history is likely to be complicated and requires future study. With some effort, the observed fractionation patterns may be used to test the hypothesis presented here.

[16] An early Mars without a dense  $\text{CO}_2$  atmosphere should have remained cold and dry. Thus, throughout most part of the early Noachian, except perhaps during relatively short periods following large volcanic outgassing or impact events, large amounts of  $\text{H}_2\text{O}$  and  $\text{CO}_2$  could have been

trapped as ices on its surface and may thereby have been protected from escape to space. After 4.1 Ga, the solar EUV energy flux should have decreased from early extreme values, and this would have led to significantly slower thermal escape of carbon from early Mars, allowing  $\text{CO}_2$  released volcanically to form a dense atmosphere. A temporary warmer climate could have released the large amount of volatiles (0.5 to several bars of  $\text{CO}_2$ ) trapped on the surface, thereby bolstering the atmospheric greenhouse effect. A warm and wet Mars could conceivably have been maintained for a few hundred Myrs in the late Noachian, during which time widespread water erosion surface features could have formed. Such a scenario corresponds well with observed features on the Martian surface.

[17] It has been hypothesized that conditions on early Mars were basically similar to those on Earth during the first several hundred Myrs of the planets’ histories [Jakosky and Phillips, 2001; McKay and Stoker, 1989], in the sense that the environments on both planets were favorable for the existence of stable liquid water. The divergence between the two planets was considered to have occurred later as a consequence of fast nonthermal escape associated with solar wind interactions after the disappearance of Mars’ intrinsic magnetic field. Our work suggests that Earth and Mars diverged at the very earliest stages of their evolutionary histories, and it highlights the importance of a planet’s mass in retaining its atmosphere and maintaining habitability.

[18] **Acknowledgments.** We thank J. M. Forbes and S. W. Bougher for providing atmospheric data of present Mars and Venus, K. Zahnle for helpful discussions, and M. J. Beach for help evaluating the mesopause conditions of early Mars. F. T. was partially supported by the NASA Postdoctoral Program through the NASA Astrobiology Institute under Cooperative Agreement CAN-00-OSS-01. J. F. K. acknowledges support from NASA Exobiology grant NNG05G088G and from the NASA Astrobiology Institute. S. C. S. acknowledges support from NASA grant NNX07AC55G to the National Center for Atmospheric Research. The National Center for Atmospheric Research is supported by the National Science Foundation.

## References

- Baker, V. R. (2001), Water and the Martian landscape, *Nature*, 412, 228.
- Canfield, D., M. T. Rosing, and C. Bjerrum (2006), Early anaerobic metabolisms, *Philos. Trans. R. Soc., Ser. B*, 361, 1819.
- Carr, M. H. (1986), Mars: A water-rich planet?, *Icarus*, 68, 187.
- Chin, G., and H. A. Weaver (1984), Vibrational and rotational excitation of CO in comets, *Astrophys. J.*, 285, 858.
- Forget, F., and R. T. Pierrehumbert (1997), Warming early Mars with carbon dioxide clouds that scatter infrared radiation, *Science*, 278, 1273.
- Fox, J. L., and K. Y. Sung (2001), Solar activity variations of the Venus thermosphere/ionosphere, *J. Geophys. Res.*, 106, 21,305–21,335.
- Glenar, D. A., E. Bleuler, and J. S. Nisbet (1978), The energy balance of the nighttime thermosphere, *J. Geophys. Res.*, 83, 5550.
- Gordiets, B. F., Y. N. Kulikov, M. N. Markov, and M. Y. Marov (1982), Numerical modeling of the thermospheric heat budget, *J. Geophys. Res.*, 87, 4504.
- Hedin, A. E., H. B. Niemann, W. T. Kasprzak, and A. Seiff (1983), Global empirical-model of the Venus thermosphere, *J. Geophys. Res.*, 88, 73–83.
- Holland, H. D. (2002), Volcanic gases, black smokers and the Great Oxidation Event, *Geochim. Cosmochim. Acta*, 66, 3811.
- Jakosky, B. M., and R. J. Phillips (2001), Mars’ volatile and climate history, *Nature*, 412, 237.
- Kasting, J. F. (1991),  $\text{CO}_2$  condensation and the climate of early Mars, *Icarus*, 94, 1.
- Kasting, J. F. (1993), Earth’s early atmosphere, *Science*, 259, 920.
- Kockarts, G. (1980), Nitric oxide cooling in the terrestrial thermosphere, *Geophys. Res. Lett.*, 7, 137.
- Krasnopolsky, V. A., *et al.* (2007), Oxygen and carbon isotope ratios in the Martian atmosphere, *Icarus*, 192, 396–403.

- McElroy, M. B. (1972), Mars: An evolving atmosphere, *Science*, *175*, 443.
- McKay, C. P., and C. R. Stoker (1989), The early environment and its evolution on Mars: Implications for life, *Rev. Geophys.*, *27*, 189.
- Melosh, H. J., and A. M. Vickery (1989), Impact erosion of the primordial Martian atmosphere, *Nature*, *338*, 487.
- Mischna, M. M., J. F. Kasting, A. A. Pavlov, and R. Freedman (2000), Influence of carbon dioxide clouds on early Martian climate, *Icarus*, *145*, 546.
- Phillips, R. J., et al. (2001), Ancient geodynamics and global-scale hydrology on Mars, *Science*, *291*, 2587.
- Ribas, I., E. F. Guinan, M. Gudel, and M. Audard (2005), Evolution of the solar activity over time and effects on planetary atmospheres. I. High-energy irradiances (1–1700 Å), *Astrophys. J.*, *622*, 680.
- Sawada, T., D. J. Strickland, and A. E. S. Green (1972), Electron energy deposition in CO<sub>2</sub>, *J. Geophys. Res.*, *77*, 4812.
- Segura, T. L., O. B. Toon, A. Colaprete, and K. Zahnle (2002), Environmental effects of large impacts on Mars, *Science*, *298*, 1977.
- Sleep, N. H., and K. Zahnle (2001), Carbon dioxide cycling and implications for climate on ancient Earth, *J. Geophys. Res.*, *106*, 1373.
- Smithro, C. G., and J. J. Sojka (2005), Behavior of the ionosphere and thermosphere subject to extreme solar cycle conditions, *J. Geophys. Res.*, *110*, A08306, doi:10.1029/2004JA010782.
- Solomon, S. C., et al. (2005), New perspectives on ancient Mars, *Science*, *307*, 1214.
- Stewart, A. I. F. (1987), Revised time dependent model of the Martian atmosphere for use in orbit lifetime and sustenance studies, *Final Rep. JPL PO NQ-802429*, Jet Propul. Lab., Pasadena, Calif.
- Tian, F., O. B. Toon, A. A. Pavlov, and H. De Sterck (2005), A hydrogen rich early Earth atmosphere, *Science*, *308*, 1014–1017.
- Tian, F., J. F. Kasting, H. Liu, and R. G. Roble (2008a), Hydrodynamic planetary thermosphere model: 1. Response of the Earth's thermosphere to extreme solar EUV conditions and the significance of adiabatic cooling, *J. Geophys. Res.*, *113*, E05008, doi:10.1029/2007JE002946.
- Tian, F., S. C. Solomon, L. Qian, J. Lei, and R. G. Roble (2008b), Hydrodynamic planetary thermosphere model: 2. Coupling of an electron transport/energy deposition model, *J. Geophys. Res.*, *113*, E07005, doi:10.1029/2007JE003043.
- Zahnle, K., R. M. Haberle, D. C. Catling, and J. F. Kasting (2008), Photochemical instability of the ancient Martian atmosphere, *J. Geophys. Res.*, *113*, E11004, doi:10.1029/2008JE003160.

---

J. F. Kasting, Department of Geosciences, Pennsylvania State University, University Park, PA 16802, USA.

S. C. Solomon, High Altitude Observatory, National Center for Atmospheric Research, 3080 Center Green, Boulder, CO 80301, USA.

F. Tian, Department of Earth, Atmospheric, and Planetary Sciences, MIT, 77 Massachusetts Avenue, Cambridge, MA 02139, USA. (tianfeng@mit.edu)